Smart Structures and Systems, Vol. 5, No. 5 (2009) 547-564
DOI: http://dx.doi.org/10.12989/sss.2009.5.5.547

Static analysis of a multilayer piezoelectric actuator with bonding layers and electrodes

H. J. Xiang* and Z. F. Shi

School of Civil Engineering, Beijing Jiaotong University, 100044, Beijing, P. R. China

(Received July 22, 2008, Accepted February 4, 2009)

Abstract. Based on the theory of piezoelasticity, an analytical solution for a typical multilayer piezoelectric composite cantilever is obtained by the *Airy* function method. The piezoelectric cantilever may consist of any number of layers. Moreover, the material and thickness for different layers may be different. The solution obtained in the present paper is concise and can be easily applied for the bending analysis of multilayer piezoelectric actuators considering the effect of bonding layers and electrodes. At last, a comprehensive parametric study is conducted to show the influence of electromechanical coupling (EMC), the number of piezoelectric layers, the elastic modulus of elastic layer and the thickness ratio on the bending behavior of actuators. Some interesting results for the design of multilayer piezoelectric actuators are presented.

Keywords: piezoelectric material; piezoelectric composite; multilayer; actuators.

1. Introduction

Due to their excellent electro-mechanical properties, easy fabrication, design flexibility, and efficiency in transforming electrical energy to mechanical energy via the inverse piezoelectric effect, piezoelectric actuators have been extensively used in a variety of applications such as micro-electro-mechanical systems (MEMS), active vibration control, compact electronic equipment, precision position control, loudspeakers, etc. Typical piezoelectric bending actuators involve multilayer stacks which have a greater sensitivity compared with single-layer element (Desmare 1999). If they are made of piezoelectric polymeric materials, these devices can also offer some advantages over piezoelectric ceramic transducers, such as flexibility, ease of preparing large sheets and the ability to undergo large deflections without damage (Marcus 1984).

Because of its advantages and wide applications, multi-layered piezoelectric structures have attracted much attention in recent years. For example, the constitutive equations for piezoelectric device are simplified as one-dimensional constitutive equations with the assumptions that the shear effects are negligible, beam thickness is much less than the piezoelectric-induced curvature, second order effects such as electrostriction are negligible, and *xy*-plane strain and *xz*-plane stress are enforced. Based on the one-dimensional constitutive equations, some simple behaviors of symmetric or non-symmetric piezoelectric cantilever bimorphs were studied (Smits, *et al.* 1991, Smits and Ballato 1994, Brissaud, *et al*. 2003, Brissaud 2004, Ballas, *et al*. 2006). Using the same constitutive equations, impedance and

*Corresponding Author, E-mail: xhjun@tom.com, zfshi178@sohu.com

admittance matrices were proposed for the analysis of the beam-type piezoelectric multi-morph devices (Ha and Kim 2002). By neglecting the effect of transverse shear on the deformation of the beam, a simple closed-form solution for the bending of piezoelectric multimorphs was obtained (Weinberg 1999) based on the Bernoulli–Euler beam theory. The fundamental assumptions in this theory are that cross sections remain plane and normal to the deformed beam axis, appropriately giving the slender geometry of some multimorphs. Moreover, in the above solution, equilibrium is imposed in a weak sense using integrals over the beam thickness. The resulting formulation is expressed in terms of effective cross section properties. With the help of the expedient coupling coefficient, Weinberg's solution (1999) was extended to arbitrary electromechanical coupling (EMC) by using a simple correction to the moment of inertia of the piezoelectric layers (Tadmor and Kósa 2003). Also based on the Bernoulli–Euler beam theory, the natural frequencies, maximum displacement and resultant force of a symmetric multi-morph cantilever were obtained (Lee, *et al.* 2005). Similar as Timoshenke's well-known derivation for thermal bimorph deflections, DeVoe and Pisano (1997) extended the approach to a cantilever multimorph, which consists of several layers of elastic or piezoelectric, but all piezoelectric layers are made of the same material. The tip deflection of the mutilayered structure was analyzed by Huang, *et al.* (2004) using a similar model in the reference (DeVoe and Pisano 1997). A lot of previous studies took the electric field in each layer of the multimorphs as a constant. As is well-known to all, in the case of bending or transverse shear, the strains through the thickness of the piezoelectric layer are usually nonuniform. If a constant electric field is assumed, the electric displacement through the thickness should not be constant. In order to improve the accuracy, a new approach for laminated plates with piezoelectric layers was proposed based on a refinement improvement of the electric potential as a function of the thickness coordinate (Fernandes and Pouget 2002). By using Timoshenko theory, the static bending, free vibration, and dynamic response of monomorph, bimorph, and multimorph actuators were investigated (Yang and Xiang 2007, Zhou, *et al.* 2005). For an intelligent beam with single elastic layer and two piezoelectric layers, a static analysis with a voltage applying on these two piezoelectric layers was performed by using *Airy* stress function method (Lin, *et al.* 2001). On the other hand, based on the Fourier series, an exact analysis for a multilayer composite with the simply supported boundary conditions was conducted (Heyliger and Brooks 1996). Most recently, the third-order displacement theory was employed and a set of cubic functions was proposed to describe the distribution of the electric potential field for a composite smart beam. And then, the problem was solved by finite element method (Wang, *et al.* 2007). It is worth to mention that Pan and his co-worker presented some exact solutions for a multilayered rectangular plate made of anisotropic and functionally graded magneto-electro-elastic materials by the pseudo-Stroh formalism and the propagator matrix method (Pan 2001, Pan and Han 2005). The method is very convenient for studying multilayered structures of which the boundary condition is simply supported.

Though there are considerable papers dealing with multilayered actuators, most of the investigations were following Timoshenko's approach or based on the elementary theory of elasticity. Moreover, it is noted that the effects of bonding layers can not be ignored in some cases. The design theory for a piezoelectric actuator was presented considering the effect of bonding layers (Marcus 1984), but the electric field was assumed as a constant. So, the objective of the present research is to give a precise analysis of the multilayer piezoelectric actuator considering the bonding layers and electrodes based on the theory of piezoelasticity. As the continuation of our previous studies where all layers of the actuator were connected in series (Xiang and Shi 2008) or only the piezoelectric coefficient g_{31} is different from layer to layer (Shi, *et al.* 2006), the present paper investigates another typical multilayer piezoelectric actuator of which all piezoelectric layers are connected in parallel. In addition, the material and thickness for different layers may be different. An exact solution for the multimorph is given, which exactly satisfies all the equilibrium conditions and continuous conditions for the stress, displacement and induction as well as electric potential on the interfaces between adjacency layers. The organization of the rest of this paper is as follows. The basic equations for piezoelectric materials are summarized in Section 2. The exact solutions for the multilayer piezoelectric composite cantilevers are obtained in Section 3. In Section 4, a comprehensive parametric study is conducted to show the influence of electromechanical coupling, the number of piezoelectric layers, the elastic modulus of elastic layer and the thickness ratio on the bending behavior of actuators.

2. Basic equations

Among the piezoelectric devices, the cantilevers are the most frequently investigated structures (Liu, *et al.* 2006, DeVoe and Pisano 1997, Smits, *et al.* 1991). As shown in Fig. 1, a multilayer piezoelectric cantilever is investigated as a structure of multimorph actuators, of which the piezoelectric layer and the elastic layer are placed alternately. There are n+1 elastic layers (electrodes or bonding layers) and n piezoelectric layers. In one implementation of these devices, all interfaces between neighboring piezoelectric layers are dielectric. Between the opposite surfaces of every piezoelectric layer there is an external electrical potential V_0. In addition, the actuator is subjected to a moment M_0 and a longitudinal force N_0 at the free end. The thickness of either elastic or piezoelectric layers may be different. Obviously, the thickness of the elastic layer k is determined by $h_{e,k} = h_{2k-1}-h_{2k-2}$ and the thickness of the piezoelectric layer k is determined by $h_{p,k} = h_{2k}-h_{2k-1}$ as shown in Fig. 1. Referring to a Cartesian coordinate system (x-0-z) and denoting ε_{ij}, σ_{ij}, D_i and E_i as the components of strain, stress, induction and electric field, respectively, the constitutive equations for transversely isotropic elastic materials and piezoelectric materials under the condition of plane deformation can be written as follows

$$\begin{cases} \varepsilon_x = S_{11Ek}\sigma_x + S_{13Ek}\sigma_z \\ \varepsilon_z = S_{13Ek}\sigma_x + S_{33Ek}\sigma_z \\ \gamma_{xz} = S_{44Ek}\tau_{xz} \end{cases} \quad \text{(in elastic layer } k\text{)} \tag{1}$$

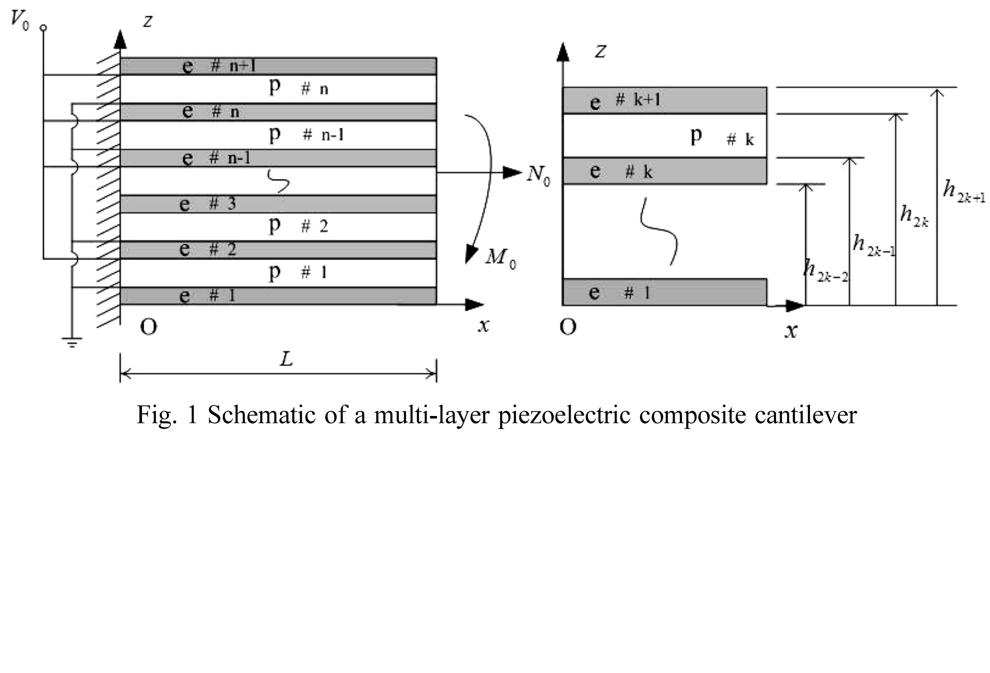

Fig. 1 Schematic of a multi-layer piezoelectric composite cantilever

$$\begin{cases} \varepsilon_x = S_{11Pk}\sigma_x + S_{13Pk}\sigma_z + g_{31k}D_z \\ \varepsilon_z = S_{13Pk}\sigma_x + S_{33Pk}\sigma_z + g_{33k}D_z \\ \gamma_{xz} = S_{44Pk}\tau_{xz} + g_{15k}D_x \\ E_x = -g_{15k}\tau_{xz} + \beta_{11k}D_x \\ E_z = -g_{31k}\sigma_x - g_{33k}\sigma_z + \beta_{33k}D_z \end{cases} \quad \text{(in piezoelectric layer } k\text{)} \tag{2}$$

where S_{ijEk} and S_{ijPk} are the coefficients of the effective elastic compliance for elastic layers and piezoelectric layers, respectively. The coefficients of the piezoelectric and dielectric impermeability for the piezoelectric layers are denoted by g_{ij} and β_{ij}, respectively. The subscript k is added in the coefficients to distinguish different layers. It should be mentioned that the above material coefficients S_{ijE}, S_{ijP}, g_{ij} and β_{ij} in the plane stress condition are the same as those in 3D case. However these coefficients should be changed in the plane strain case, which is detailed in the reference (Xiang 2007). The strain components for both elastic and piezoelectric materials can be expressed by means of the displacement components (u and w) as

$$\varepsilon_x = \frac{\partial u}{\partial x}, \varepsilon_z = \frac{\partial w}{\partial z}, \gamma_{xz} = \frac{\partial u}{\partial z} + \frac{\partial w}{\partial x} \tag{3}$$

For piezoelectric materials, there is another set of equations between the electric field and the electrical potential φ as

$$E_x = \frac{\partial \phi}{\partial x}, E_z = -\frac{\partial \varphi}{\partial z} \tag{4}$$

Without consideration of body force the static equilibrium equations for both elastic and piezoelectric materials can be given as

$$\frac{\partial \sigma_x}{\partial x} + \frac{\partial \tau_{xz}}{\partial z} = 0, \frac{\partial \tau_{xz}}{\partial x} + \frac{\partial \sigma_z}{\partial z} = 0 \tag{5}$$

On the other hand, without consideration of body charge, the induction components in the piezoelectric materials should satisfy the following Maxwell's equation

$$\frac{\partial D_x}{\partial x} + \frac{\partial D_z}{\partial z} = 0 \tag{6}$$

To ensure that the displacement and electric potential can be obtained by integrating Eqs. (3) and (4), the components of strain and electric field must satisfy the following equations

$$\frac{\partial^2 \varepsilon_x}{\partial z^2} + \frac{\partial^2 \varepsilon_z}{\partial x^2} = \frac{\partial^2 \gamma_{xz}}{\partial x \partial z}, \frac{\partial E_x}{\partial z} - \frac{\partial E_z}{\partial x} = 0 \tag{7}$$

Under the consideration of some detailed boundary conditions, these basic equations will be solved in the following sections.

3. Exact solution based on the *Airy* stress function method

To find the solution of the basic equations, the *Airy* stress function method is used in the present paper. As is easily checked, Eqs. (5) and (6) are satisfied by introducing a stress function $\tilde{\varphi}$ and an induction function ψ and putting the following expressions for stress components and induction components

$$\begin{cases} \sigma_x = \dfrac{\partial^2 \tilde{\varphi}}{\partial z^2}, \sigma_z = \dfrac{\partial^2 \tilde{\varphi}}{\partial x^2}, \tau_{xz} = -\dfrac{\partial^2 \tilde{\varphi}}{\partial x \partial z} \\ D_x = \dfrac{\partial \psi}{\partial z}, D_z = -\dfrac{\partial \psi}{\partial x} \end{cases} \tag{8}$$

In this manner we can get a variety of solutions of the equation of equilibrium Eq. (5) and the Maxwell's Eq. (6). The true solution of the problem is that which satisfies also the compatibility Eq. (7) and all boundary conditions. It is noted that this paper just considers the plane problem of an anisotropic beam which the material composition varies continuously in the direction of the thickness, so the stress functions $\tilde{\varphi}_{Ek}$, $\tilde{\varphi}_{Pk}$ and the induction function ψ_k of layer k are assumed as:

$$\tilde{\varphi}_{Ek} = -a_{Ek} z^3 + b_{Ek} z^2 \qquad \text{(for elastic layer } k\text{)} \tag{9}$$

$$\tilde{\varphi}_{Pk} = -a_{Pk} z^3 + b_{Pk} z^2,\ \psi_k = l_k x \qquad \text{(for piezoelectric layer } k\text{)} \tag{10}$$

where a_{Ek}, b_{Ek}, a_{Pk}, b_{Pk} and l_k are constants to be determined by boundary conditions. The stress function $\tilde{\varphi}_{Ek}$ (or $\tilde{\varphi}_{Pk}$) is taken as assumed to be a third-order polynomial function of z instead of a high order polynomial function. The reason is that the third-order polynomial stress function is enough to give a solution which all boundary conditions can be satisfied as what we can see as follows. If some new unknown constants, such as c and d (or more), are added in the Airy stress function ($-az^3 + bz^2 + cz^4 + dz^5$) to obtain a high order polynomial function, we will find that these constants c and d must be zero once the boundary conditions are satisfied. By using of the stress functions $\tilde{\varphi}_{Ek}$, $\tilde{\varphi}_{Pk}$ and the induction function ψ_k, the components of stress and induction in the layer k can be obtained as

$$\begin{cases} \sigma_x = -6a_{Ek} z + 2b_{Ek} \\ \sigma_z = \tau_{xz} = 0 \end{cases} \qquad \text{(in elastic layer } k\text{)} \tag{11}$$

$$\begin{cases} \sigma_x = -6a_{Pk} z + 2b_{Pk},\ \sigma_z = \tau_{xz} = 0 \\ D_x = 0, D_z = -l_k \end{cases} \qquad \text{(in piezoelectric layer } k\text{)} \tag{12}$$

From Eqs. (1), (2) (11) and (12), it is easily verified that Eq. (7) is satisfied. Further, by the use of Eqs. (1), (2), (3) and (4) the displacement and electrical potential in layer k can be derived as follows

$$\begin{cases} u = -6a_{Ek} S_{11Ek} xz + 2b_{Ek} S_{11Ek} x + \omega_{Ek} z + u_{Ek} \\ w = -3a_{Ek} S_{13Ek} z^2 + 2b_{Ek} S_{13Ek} z + 3a_{Ek} S_{11Ek} x^2 - \omega_{Ek} x + w_{Ek} \end{cases} \qquad \text{(in elastic layer } k\text{)} \tag{13}$$

$$\begin{cases} u = -6a_{Pk}S_{11Pk}xz + 2b_{Pk}S_{11Pk}x - g_{31k}l_{Pk}x + \omega_{Pk}z + u_{Pk} \\ w = -3a_{Pk}S_{13Pk}z^2 + 2b_{Pk}S_{13Pk}z - g_{33k}l_{Pk}z + 3a_{Pk}S_{11Pk}x^2 - \omega_{Pk}x + w_{Pk} \\ \varphi = -3a_{Pk}g_{31k}z^2 + 2b_{Pk}g_{31k}z + \beta_{33k}l_{Pk}z + \varphi_k \end{cases} \text{(in piezoelectric layer } k\text{)} \quad (14)$$

where a_{Pk}, a_{Ek}, b_{Pk}, b_{Ek}, l_{Pk}, ω_{Pk}, ω_{Ek}, u_{Pk}, u_{Ek}, w_{Pk}, w_{Ek}, φ_k are constants to be determined by using geometrical and electrical boundary conditions. To find the exact solution of the multi-layered piezoelectric cantilever, the solutions expressed by Eqs. (11)-(14) should be correctly assembled by considering some boundary conditions and continuous conditions at the interfaces. It is obvious that the following boundary conditions are satisfied automatically

$$D_x = 0 \quad \text{at} \quad x = 0, L \quad (15)$$

$$\tau_{xz} = 0 \quad \text{at} \quad x = L \quad (16)$$

$$\sigma_z = 0, \quad \tau_{xz} = 0 \quad \text{at} \quad z = 0 \text{ and } z = h_{2n+1} \quad (17)$$

Besides, the continuous conditions for the stresses at the interfaces are also satisfied automatically. On the other hand, the displacements at the interfaces should be continuous, i.e.

$$\begin{cases} u(x, h_{i-}) = u(x, h_{i+}) \\ w(x, h_{i-}) = w(x, h_{i+}) \end{cases}, \quad 1 \le i \le 2n \quad (18)$$

which leads to the following equations

$$\begin{cases} u(x, h_{2k-1}) = -6a_{Ek}S_{11Ek}xh_{2k-1} + 2b_{Ek}S_{11Ek}x + \omega_{Ek}h_{2k-1} + u_{Ek} \\ \qquad = -6a_{Pk}S_{11Pk}xh_{2k-1} + 2b_{Pk}S_{11Pk}x - g_{31k}l_kx + \omega_{Pk}h_{2k-1} + u_{Pk}, \\ u(x, h_{2k}) = -6a_{E,k+1}S_{11E,k+1}xh_{2k} + 2b_{E,k+1}S_{11E,k+1}x + \omega_{E,k+1}h_{2k} + u_{E,k+1} \\ \qquad = -6a_{Pk}S_{11Pk}xh_{2k} + 2b_{Pk}S_{11Pk}x - g_{31k}l_kx + \omega_{Pk}h_{2k} + u_{Pk}, \\ w(x, h_{2k-1}) = -3a_{Ek}S_{13Ek}h_{2k-1}^2 + 2b_{Ek}S_{13Ek}h_{2k-1} + 3a_{Ek}S_{11Ek}x^2 - \omega_{Ek}x + w_{Ek} \\ \qquad = -3a_{Pk}S_{13Pk}h_{2k-1}^2 + 2b_{Pk}S_{13Pk}h_{2k-1} - g_{33k}l_kh_{2k-1} + 3a_{Pk}S_{11Pk}x^2 - \omega_{Pk}x + w_{Pk}, \\ w(x, h_{2k}) = -3a_{E,k+1}S_{13E,k+1}h_{2k}^2 + 2b_{E,k+1}S_{13E,k+1}h_{2k} + 3a_{E,k+1}S_{11E,k+1}x^2 - \omega_{E,k+1}x + w_{E,k+1} \\ \qquad = -3a_{Pk}S_{13Pk}h_{2k}^2 + 2b_{Pk}S_{13Pk}h_{2k} - g_{33k}l_kh_{2k} + 3a_{Pk}S_{11Pk}x^2 - \omega_{Pk}x + w_{Pk}. \end{cases} \quad (19)$$

for k from 1 to n. From Eq. (19), the following relationships can be obtained

$$\omega_{Ek} = \omega_{Pk} = \omega_0, u_{Ek} = u_{Pk} = u_0 \quad (20)$$

$$a_{Pk}S_{11Pk} = a_{Ek}S_{11Ek} = a_{P1}S_{11P1} \quad (21)$$

$$2b_{Ek}S_{11Ek} = 2b_{Pk}S_{11Pk} - g_{31k}l_k = 2b_{P1}S_{11P1} - g_{311}l_1 \quad (22)$$

Here u_0 and ω_0 are constants to be determined. We also obtain the following $2n$ equations, which can be used to determine w_{P1}, w_{P2},..., w_{Pn} and w_{E1}, w_{E2},..., $w_{E,n+1}$ once one of them is known

$$\begin{cases} -3a_{Ek}S_{13Ek}h_{2k-1}^2 + 2b_{Ek}S_{13Ek}h_{2k-1} + w_{Ek} \\ \quad = -3a_{Pk}S_{13Pk}h_{2k-1}^2 + 2b_{Pk}S_{13Pk}h_{2k-1} - g_{33k}l_kh_{2k-1} + w_{Pk} \\ -3a_{E,k+1}S_{13E,k+1}h_{2k}^2 + 2b_{E,k+1}S_{13E,k+1}h_{2k} + w_{E,k+1} \\ \quad = -3a_{Pk}S_{13Pk}h_{2k}^2 + 2b_{Pk}S_{13Pk}h_{2k} - g_{33k}l_kh_{2k} + w_{Pk} \end{cases} \tag{23}$$

The electrical boundary conditions are

$$\varphi(x, h_{2k-1}) = 0, \varphi(x, h_{2k}) = V_0, (1 \le k \le n) \tag{24}$$

which lead to

$$\varphi_k = 3a_{pk}g_{31k}h_{2k-1}^2 - 2b_{Pk}g_{31k}h_{2k-1} - \beta_{33k}l_kh_{2k-1} \tag{25}$$

$$\begin{aligned} V_0 &= -3a_{Pk}g_{31k}(h_{2k}^2 - h_{2k-1}^2) + 2b_{Pk}g_{31k}(h_{2k} - h_{2k-1}) + \beta_{33k}l_k(h_{2k} - h_{2k-1}) \\ &= -3a_{P1}g_{311}(h_2^2 - h_1^2) + 2b_{P1}g_{311}(h_2 - h_1) + \beta_{331}l_1(h_2 - h_1) \end{aligned} \tag{26}$$

From Eqs. (21), (22) and (26), the constants (a_{Ek}, b_{Ek}) and (a_{Pk}, b_{Pk}, l_k) can be expressed in terms of (a_{P1}, b_{P1}, l_1) as follows

$$(a_{Ek}, b_{Ek})^T = A^{(k)}(a_{P1}, b_{P1}, l_1)^T \tag{27}$$

$$(a_{Pk}, b_{Pk}, l_k)^T = (\tilde{R}^{(k)})^{-1}\tilde{R}^{(1)}(a_{P1}, b_{P1}, l_1)^T = R^{(k)}(a_{P1}, b_{P1}, l_1)^T \tag{28}$$

where vectors with superscript 'T' denote the transpose of the vector. The matrix $R^{(k)} = (\tilde{R}^{(k)})^{-1}\tilde{R}^{(1)}$ which is a 3×3 matrix and the matrixes $A^{(k)}$ and $\tilde{R}^{(k)}$ are listed in Appendix. Introducing a matrix $B^{(k)}$ and a vector $C^{(k)}$ as

$$B^{(k)} = \begin{pmatrix} r_{11}^{(k)} & r_{12}^{(k)} & r_{13}^{(k)} \\ r_{21}^{(k)} & r_{22}^{(k)} & r_{23}^{(k)} \end{pmatrix}, C^{(k)} = (r_{31}^{(k)} \; r_{32}^{(k)} \; r_{33}^{(k)}) \tag{29}$$

where $r_{ij}^{(k)}$ are the elements of matrix $R^{(k)}$, the following relationships can be obtained

$$(a_{Pk}, b_{Pk}) = B^{(k)}(a_{P1}, b_{P1}, l_1)^T \tag{30}$$

$$l_k = C^{(k)}(a_{P1}, b_{P1}, l_1)^T \tag{31}$$

From Eqs. (25), (27), (30) and (31), it is found that the constants a_{Pk}, b_{Pk}, a_{Ek}, b_{Ek}, l_k and φ_k will be determined if the constants a_{P1}, b_{P1} and l_1 are given. In order to find the constants a_{P1}, b_{P1} and l_1, the Saint-Venant's principle is considered as the following mechanical boundary conditions at the free end ($x = L$) of the cantilever

$$\begin{cases} \sum_{k=1}^{n} \int_{h_{2k-1}}^{h_{2k}} (-6a_{Pk}z + 2b_{Pk})dz + \sum_{k=1}^{n+1} \int_{h_{2k-2}}^{h_{2k-1}} (-6a_{Ek}z + 2b_{Ek})dz = N_0 \\ \sum_{k=1}^{n} \int_{h_{2k-1}}^{h_{2k}} (-6a_{Pk}z + 2b_{Pk})zdz + \sum_{k=1}^{n+1} \int_{h_{2k-2}}^{h_{2k-1}} (-6a_{Ek}z + 2b_{Ek})zdz = M_0 \end{cases} \tag{32}$$

For simplicity, denote $\eta = (a_{P1}, b_{P1}, l_1)^T$. Keeping Eqs. (27) and (30) in mind, Eqs. (26) and (32) can be written in matrix form as

$$K\eta = (N_0, M_0, V_0)^T \tag{33}$$

and thus

$$\eta = K^{-1}(N_0, M_0, V_0)^T \tag{34}$$

where $K = [k_{ij}]_{3\times 3}$ whose elements are listed in Appendix. Then we can obtain the exact solutions for stress and induction in the layer k from Eqs. (11) and (12) as follows

$$\begin{cases} \sigma_x = [-6z, 2]A^{(k)}\eta \\ \sigma_z = \tau_{xz} = 0 \end{cases} \quad \text{(in elastic layer } k\text{)} \tag{35}$$

$$\begin{cases} \sigma_x = [-6z, 2]B^{(k)}\eta \\ \sigma_z = \tau_{xz} = 0 \\ D_x = 0, D_z = -C^{(k)}\eta \end{cases} \quad \text{(in piezoelectric layer } k\text{)} \tag{36}$$

In order to determine the parameters u_0, ω_0, w_{Ek} and w_{Pk}, the displacement boundary conditions at the clamp end ($x = 0$) of the cantilever are considered as

$$u(0, h_{2I-1}) = 0, w(0, h_{2I-1}) = 0, \frac{\partial w(0, h_{2I-1})}{\partial w} = 0. \ (I \in \{1, 2, 3, \ldots, n\}) \tag{37}$$

which leads to

$$\begin{cases} u_0 = 0, \omega_0 = 0 \\ w_{EI} = S_{13EI}h_{2I-1}[3h_{2I-1}, -2]A^{(I)}\eta \end{cases} \tag{38}$$

From Eq. (23), it is easy found that the relationship between $w_{E,i+1}$ and $w_{E,i}$

$$w_{E,i+1} - w_{E,i} = G^{(i)}\eta \tag{39}$$

for i=1, 2,…, n and the matrixes $G^{(i)}$ are given in Appendix. From Eq. (39), the constants w_{Ek} are obtained

$$w_{Ek} = \begin{cases} w_{EI} - \sum\limits_{i=k}^{I-1} G^{(i)}\eta, & k < I \\ w_{EI}, & k = 1 \\ w_{EI} + \sum\limits_{i=I}^{k-1} G^{(i)}\eta, & k > 1 \end{cases} \tag{40}$$

From Eqs. (23) and (40), the parameters w_{Pk} can be found as

$$w_{Pk} = Q^{(k)}\eta + w_{Ek} \tag{41}$$

where $Q^{(k)} = S_{13Ek}h_{2k-1}[-3h_{2k-1}, 2]A^{(k)} - h_{2k-1}[-3S_{13Pk}h_{2k-1}, 2S_{13Pk}, -g_{33k}]R^{(k)}$. Till now all the unknown parameters introduced in this section have been determined. For simplicity, we define some coefficients as $\lambda_{E,k} = S_{11Ek}/S_{13Ek}$, $\lambda_{P,k} = S_{11Pk}/S_{13Pk}$, $\gamma_{1,k} = g_{31k}/S_{11Pk}$, and $\gamma_{2,k} = g_{33k}/S_{13Pk}$. From Eqs. (13) and (14), the displacements and voltage in each layer of the actuator can be expressed as

$$\begin{cases} u = S_{11Ek}x[-6z, 2]A^{(k)}\eta \\ w = S_{13Ek}[3(\lambda_{E,k}x^2 - z^2), 2z]A^{(k)}\eta + w_{Ek} \end{cases} \tag{42}$$

for elastic layer k and

$$\begin{cases} u = S_{11Pk}x[-6z, 2, -\gamma_{1,k}]R^{(k)}\eta \\ w = S_{13Pk}[3(\lambda_{P,k}x^2 - z^2), 2z, -\gamma_{2,k}z]R^{(k)}\eta + w_{Pk} \\ \varphi = [-3g_{31k}(z^2 - h_{2k-1}^2), 2g_{31k}(z - h_{2k-1}), \beta_{33k}(z - h_{2k-1})]R^{(k)}\eta \end{cases} \tag{43}$$

for piezoelectric layer k. From Eq. (42), the tip deflection of the actuator can be developed as

$$\delta = w(L, 0) = 3S_{11P1}a_{P1}L^2 + w_{E1} \tag{44}$$

Till now, the solution of the multilayer actuator is obtained. Note that the polarization of piezoelectric layer is assumed parallel to the axis z+ in the above solution. When the polarization of a piezoelectric layer is not parallel to the axis z+, but anti-parallel to the axis z+, the piezoelectric coefficients g_{ij} should be multiplied by a minus sign (-1), while all other coefficients remain the same (Smith, *et al*. 1991, Cheng, *et al*. 2005). In the next section, a comprehensive parametric study will be conducted to highlight the influence of bonding layers or electrodes on the static behavior of the actuator by using the above solution.

4. Static behavior of multimorphs

Commonly, $d_{31}<0$ and $d_{33}>0$, that is if the electric field is applied in parallel with the polarization of the piezoelectric layer, by convention along the z-axis, the layer will tend to contract in the planes perpendicular to the applied field, that is the x and y planes, and expand along the field axis, z. Conversely, if the electric field is applied in the direction anti-parallel with the polarization of the piezoelectric layer, it will tend to expand along the planes perpendicular to the field, and contract along the direction of the field. That some layers are contracted and some layers are expanded along x-axis leads to the bending of multimorphs. There are a lot of factors influencing the bending behavior of multimorphs. Effect of electromechanical coupling (EMC), the number of piezoelectric layers, the elastic modulus of elastic layer and the thickness ratio on the bending behavior of multimorphs will be studied. In this section, discussions will be focused on the deflection or tip deflection of an actuator. In what follows, we only consider the plane strain case where the actuator is subjected to 100V voltage, i.e. $N_0 = 0$, $M_0 = 0$ and $V_0 = 100$ V as shown in Fig. 1. As a special case, for simplicity, the thickness of each elastic layer takes the same thickness as h_e and the thicknesses of all piezoelectric layers are equal to h_p in the following examples.

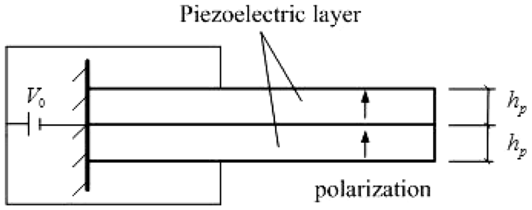

Fig. 2 Schematic of a bimorph

4.1. Effect of electromechanical coupling (EMC)

In the above solution procedure, the elastic layer and the piezoelectric layer are arranged layer wise. Note that the stress function Eq. (9) and the induction function Eq. (10) can be applied to the case that the elastic layer and the piezoelectric layer are arranged arbitrarily. The solution procedure is similar to the method used in this paper. Of course, the present solution can be used for the above-mentioned case, but it needs some modifications. For example, one piezoelectric layer will become an elastic layer when the piezoelectric coefficient of the layer is zero. On the other hand, assuming the thickness of an elastic layer to be zero, the elastic layer will be vanished and then, as a special case, the above solution can be used for a 'pure' piezoelectric multilayer beam, of which all layers are piezoelectric materials. Keeping this rule in mind and considering a parallel bimorph (Smits, *et al.* 1991) whose two piezoelectric layers are made of the same material and have the same thickness h_p as shown in Fig. 2, the tip deflection of the bimorph subjected to a voltage only is obtained from Eq. (44)

$$\delta_1 = -\frac{3S_{11P}g_{31}V_0L^2}{h_p^2(4S_{11P}\beta_{33}+g_{31}^2)} \tag{45}$$

As indicated by Eq. (43), the electric field $E_z = -\partial\varphi/\partial z$ in each piezoelectric layer is a linear function of z, instead of a constant. However, for simplicity, one of the assumptions in most of the previous studies is that the electric field in each piezoelectric layer is constant. This approximation is valid for the materials with small electromechanical coupling coefficients. Many piezoelectric materials satisfy this condition. However, modern piezoelectric materials with large coupling coefficients are designed to maximize the transfer of energy (Park and Shrout 1997). As an example, the tip deflection of the bimorph is different between present exact solution (see Eq. (45)) and the approximated solution (see Eq. (46)) based on the Euler–Bernoulli beam theory and with the assumption that the electric field in each piezoelectric layer is a constant (Smits, *et al.* 1991).

$$\delta_2 = -\frac{3d_{31}V_0L^2}{4h_p^2} \tag{46}$$

As is well-known to all, the piezoelectric coefficient $d_{31} = g_{31}/\beta_{33}$ for plane stress case and $d_{31}\approx g_{31}/\beta_{33}$ for plane strain case. Keeping this relationship in mind and considering $g_{31}^2 \ll 4S_{11P}\beta_{33}$ for many piezoelectric materials, Eq. (45) can be approximated as Eq. (46). In order to give an explanation clearly, a bimorph made of $BaTiO_3$ and another bimorph made of PZT-5A are considered herein. The material coefficients of $BaTiO_3$ are S_{11P}=7.587×10^{-12}m^2/N, g_{31}=-7.035×10^{-3}V.m/N and β_{33}=6.956 ×10^{7}m/F. Correspondingly, these material coefficients of PZT-5A are S_{11P}=10.373×10^{-12}m^2/N, g_{31}= -17.407×10^{-3} V.m/N and β_{33}=7.540×10^{7}m/F (Wang, *et al*. 1983). Take the thickness of each layer and

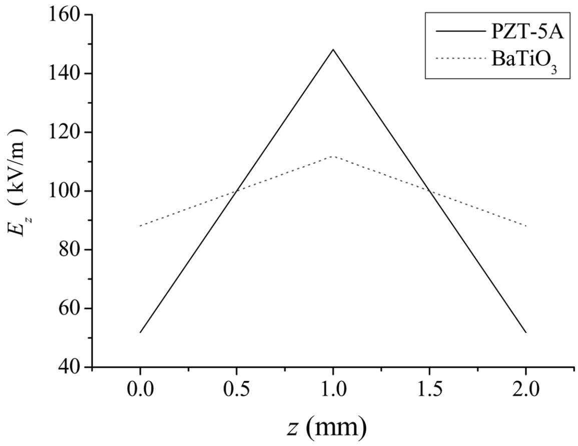

Fig. 3 Electric field E_z (absolution) distributed in a bimorph along z-axis

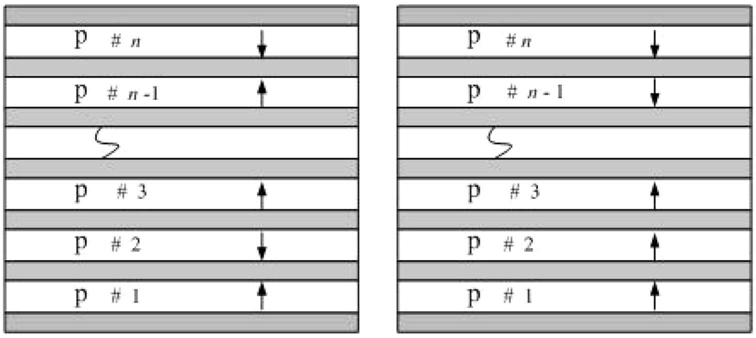

a) Case A *b*) Case B

Fig. 4 Two kinds of arrangements of polarization

length of the actuator as h_p=1 mm, L=16 mm. When the external voltage V_0 is 100V, the tip deflections δ_1 and δ_2 are 1.90 um and 1.94 um for the former bimorph, and 4.04 um and 5.43 um for the latter bimorph. The relative error $100\%\times|(\delta_2-\delta_1)/\delta_1|$ is 2.34% and 9.69% for the former and the latter bimorph, respectively. That is to say that the error can not be neglected when the piezoelectric coefficient of the material is large enough. In addition, the absolution of electric fields $E_z = -\partial\varphi/\partial z$ for the above two kinds of bimorphs are shown in Fig. 3. It is found that the electric field is not a constant, and the average of electric field, i.e. $h_p^{-1}\int E_z dz$, is 100 kV/m in each layer, which is just equal to the constant V_0/h_p assumed for electric field in the referent (Smits, *et al.* 1991).

Now, consider a multimorph with 4 piezoelectric layers made of $BaTiO_3$ and 5 electrodes made of Platinum (Pt), i.e. n = 4. As shown in Fig. 4a, the electric field E_z is anti-parallel to the polarization in 1# and 3# piezoelectric layers and parallel to the polarization in 2# and 4# piezoelectric layers when the actuator is subjected to a voltage shown in Fig. 1. The elastic modulus Y and Poisson's ratio v of the electrodes (Pt) are 171 GPa and 0.39, respectively. The material coefficients S_{ij} for the electrodes used in this paper can be determined from the above elastic modulus and Poisson's ratio, for example, $S_{11} = S_{33} = (1-v^2)/Y$, $S_{13} = -v(1+v)/Y$, $S_{44} = 2(1+v)/Y$ for isotropic materials under the plane strain condition. Besides the coefficients S_{11P}, g_{31} and β_{33} (as given above), others coefficients of $BaTiO_3$ are S_{13P}=2.599×10^{-12}m^2/N, S_{33P}=6.679×10^{-12}m^2/N, S_{44P}=17.532×10^{-12}m^2/N, g_{15}=-20.261×10^{-3}V.m/N, g_{33}=11.487×

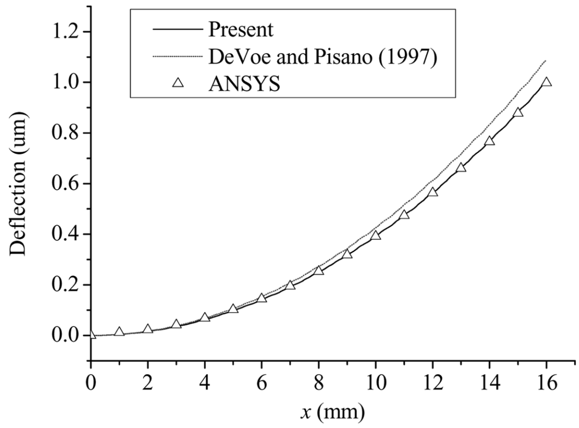

Fig. 5 The deflection of a multimorph (n=4)

10^{-3}V.m/N and β_{11}=7.793×10^7m/F (Wang, *et al.* 1983). The thicknesses of each piezoelectric layer and electrode layer are 0.5 mm and 0.1 mm, respectively. The deflections of the multimorph obtained by the present solution are plotted in Fig. 5. The results calculated by the Eq. (12) in Ref. (DeVoe and Pisano 1997) are also plotted in the figure. It is found that the present results are slightly smaller than those of DeVoe and Pisano's because of the EMC neglected by DeVoe and Pisano. For comparison, the numerical results obtained by ANSYS with element PLANE223 for piezoelectric layer and PLANE183 for elastic layer are also plotted in the same figure. Good agreements between the present analytical results and the numerical results are achieved.

4.2. Effect of the number of layers

Piezoelectric multimorphs come in different types due to differences in manufacturing methods. Two kinds of multimorphs are considered herein, as shown in Fig. 4. In Case A, the electric field E_z is anti-parallel to the polarization in odd piezoelectric layers and is parallel to the polarization in even piezoelectric layers. By contrast, in Case B, the electric field E_z is parallel to the polarization in the upper $n/2$ piezoelectric layers and is anti-parallel to the polarization in the lower $n/2$ piezoelectric layers (n is assumed as an even number here). Our focus is on the effect of the total number of piezoelectric layers on the electro-mechanical characteristics of multimorphs. In what follows, unless otherwise stated, the piezoelectric layers are $BaTiO_3$ and the elastic layers are Platinum (Pt), and each piezoelectric layer has the same thickness h_p, each elastic layer has the same thickness h_e and the ratio h_e/h_p is kept as h_e/h_p=0.2.

First, the total thickness h of the cantilever multimorph is kept as a constant, leading to $h_p=5h/(6n+1)$ and $h_e = h/(6n+1)$. Fig. 6a shows the change of the tip deflection of the multimorph versus the number of piezoelectric layers n on the condition that the total thickness h = 2 mm. The tip deflection is increased when n increases from 2 to 14 layers. The tip deflection of the 14-layer multimorph is 7.4 times that of the 2-layer bimorph for Case B while the tip deflection is increased by only 20.6% for Case A. As the total number of layers increases, the thickness of each layer is decreased and then the electric field in each layer increases rapidly. This is the main reason for which the tip deflection increases with n. On the other hand, the extended layer and the contracted layer are alternate in Case A, which results in a smaller tip deflection. However, because the extended layers and the contracted layers are distributed respectively at two sides of the center line of the multimorph in Case B, the bending of the actuator will be enhanced

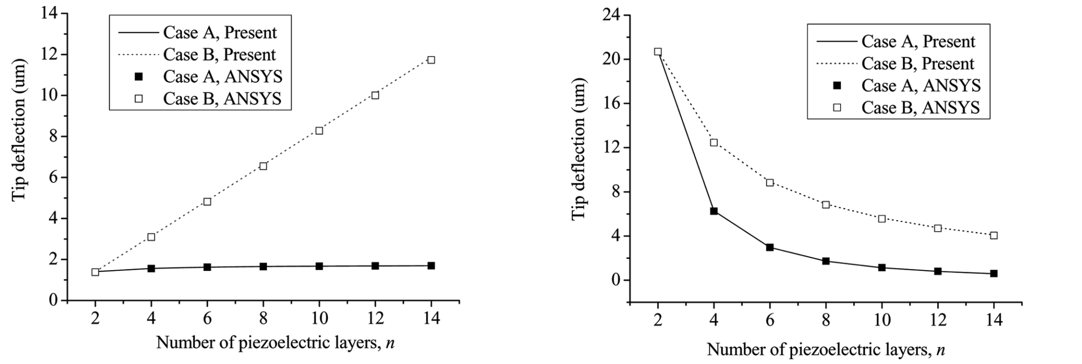

a) Total thickness of the multimorph is a constant (h = 2 mm) b) The thickness of each piezoelectric layer is a constant (h_p = 0.2mm)

Fig. 6 The tip deflection of multimorphs v.s the number of piezoelectric layers

significantly when the electric field increases. This is why the tip deflection of Case B is larger than that of Case A under the same conditions. For comparison, the results calculated by ANSYS are also plotted in Fig. 6a.

Now, let's assume that the thickness of each piezoelectric layer h_p is kept as a constant, i.e., $h = h_p(6n+1)/5$ and $h_e = 0.2h_p$. Fig. 6b shows the variation in the tip deflection of the multimorph obtained by present solution and by ANSYS when the number of piezoelectric layers n is varied and h_p= 0.2 mm. Contrary to the previous case where the total thickness is constant, the tip deflection is decreased for large layer numbers n if the thickness of each piezoelectric layer h_p is kept as a constant. The tip deflections of the 14-layer multimorph for Case A and Case B are only about 2.8% and 19.8%, respectively, of those of the 2-layer bimorphs counterparts. The bending stiffness of the actuator increases rapidly with the total thickness, but the electric field in each layer is almost invariant, so the tip deflection is decreased.

4.3. Effect of the elastic modulus of elastic layers

Consider a multimorph with h_p = 0.2 mm, h_e = 0.04 mm, n = 8 and the Poisson's ratio of elastic layer is kept as v = 0.39. As shown in Fig. 7, the tip deflection decreases monotonically with the elastic modulus

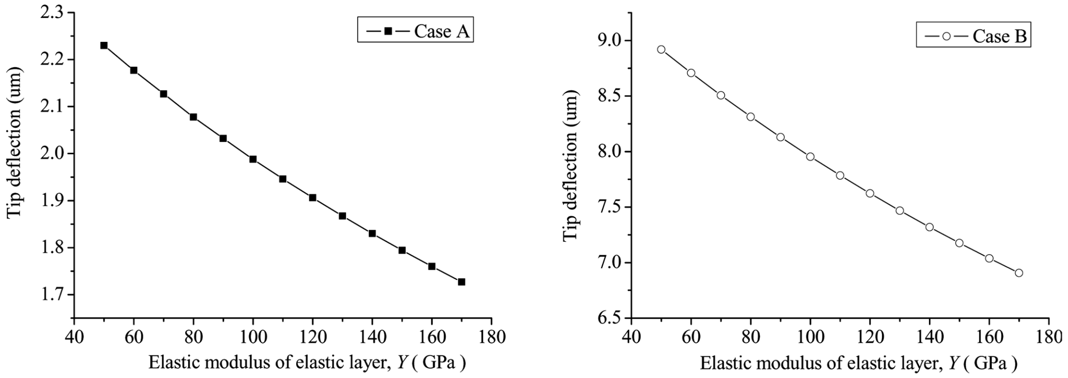

a) Case A b) Case B

Fig. 7 The effect of elastic modulus of elastic layer on the tip deflection of the multimorph (n=8)

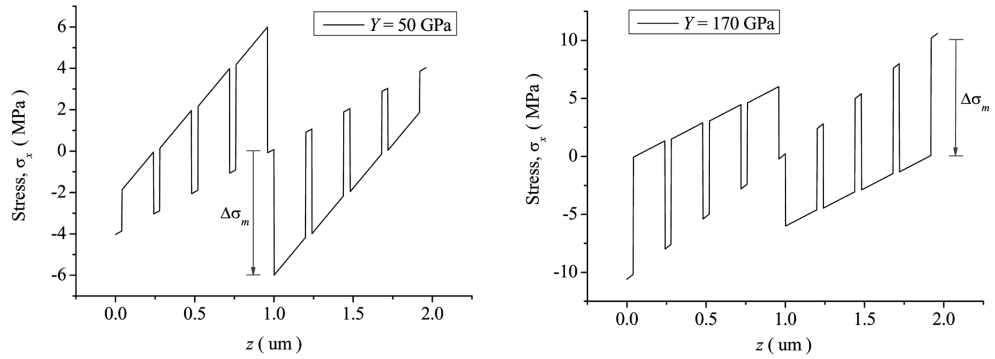

a) Elastic modulus of elastic layer Y = 50 GPa *b*) Elastic modulus of elastic layer Y = 170 GPa

Fig. 8 The normal stress σ_x distributed along z-axis (n = 8, Case B)

Y of elastic layer because the bending stiffness of the multimorph increases with the elastic modulus Y of elastic layer. The results for Case A and Case B are quite similar. They all decrease by 22.6% when the elastic modulus Y of elastic layer is changed from 50GPa to 170GPa. The only difference is the values of tip deflections for the two cases. Though there is a larger tip deflection at smaller Y of elastic layer, note that the best choice is not to design an actuator with smaller elastic modulus of elastic layer because the stiffness of the elastic layer is needed to high enough. In addition, the maximum stress difference $\Delta\sigma_m = \max_{i=1\ldots 2n}|\sigma_x(h_{i+})-\sigma_x(h_{i-})|$ near the interlayer surfaces should not be too large because of the abrupt changes in both their material composition and electro-elastic properties, which can cause severe deterioration in both the interlayer bonding strength and the response performance. Under repeated strain reversals, the high stress difference is also very likely to be the cause of premature failure. As an example, for Case B, the maximum stress difference is 5.91MPa near the center of the actuator as shown in Fig. 8a, when the elastic modulus Y of elastic layer is 50GPa. However, the maximum stress difference is 10.23MPa when the elastic modulus of elastic layer is 170GPa near the surface of the actuator as shown in Fig. 8b. When the elastic modulus Y of elastic layer is changed from 50GPa to 170GPa, the maximum stress differences for both Case A and Case B are shown in Fig. 9. It is found that the maximum stress difference is not always a monotonic function of the elastic modulus of elastic layer. For Case A, $\Delta\sigma_m$ becomes lower as the elastic modulus of elastic layer increases, and does not change

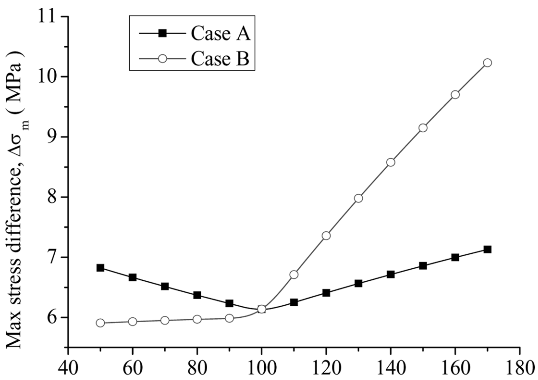

Fig. 9 The max stress difference near the interlayer surfaces varied with the elastic modulus of elastic layer (n=8)

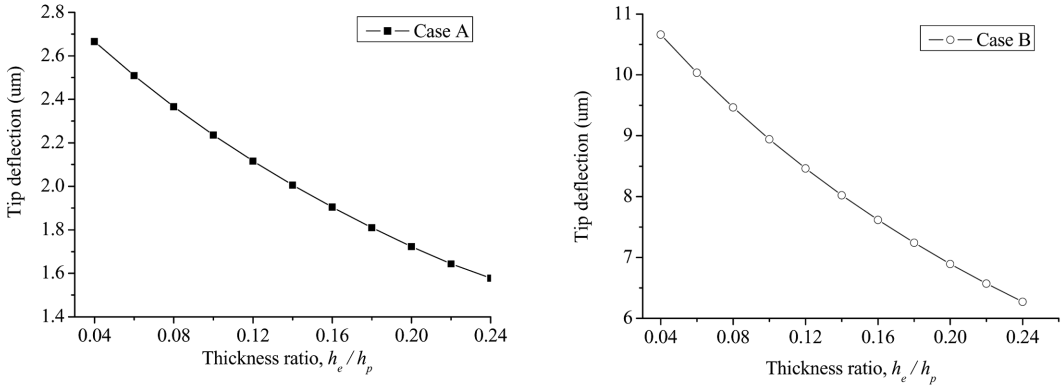

a) Case A

b) Case B

Fig. 10 Effect of the thickness ratio h_e/h_p on the tip deflection of the multimorphs (n=8)

monotonically. For example, the multimorph with an elastic modulus of elastic layer near Y = 100GPa generates the minimum $\Delta\sigma_m$. For Case B, there is an inflection point near Y = 100GPa. That is to say that the maximum stress difference of the multimorph increases steadily as Y changes from 50GPa to 100GPa, but increases rapidly after Y = 100GPa. Note that the value 100GPa is very close to the effective elastic modulus of $BaTiO_3$ which is 115GPa. Please see the reference (Li, *et al.* 1999), which gives a method to calculate the effective elastic modulus of piezoelectric material. From this point, the best multimorph should be the one whose elastic modulus of elastic layer is approximate to that of the piezoelectric layer so as to weaken the mismatch of material properties between layers. From a comprehensive point, the best design is a balance between the stress difference and the tip deflection.

4.4. Effect of the ratio h_e/h_p

Keep the thickness of piezoelectric layer as a constant h_p = 0.2 mm while changing the thickness of elastic layer h_e, so the ratio h_e/h_p is varied. Fig. 10 discusses the effects of the ratio on the tip deflection of the multimorph with n = 8. When the ratio h_e/h_p changes from 0.04 to 0.24, the tip deflection of the actuator is decreased from 2.666 um to 1.578 um for Case A, and from 10.664 um to 6.272 um for Case B, which indicates that the ratio h_e/h_p is an important factor for the bending behavior of multilayer actuators. The best actuator should be the one with thin elastic layer (including electrodes and bonding layers).

5. Conclusions

Based on the theory of piezoelasticity, the static exact solution of a multilayer piezoelectric composite cantilever is obtained by *Airy* function method. It is found that except stress component σ_x and induction component D_z, other stress and induction components disappear from the multi-layer piezoelectric composite cantilevers when they are subjected to a electric potential, a moment and a longitudinal force at free end. By using the present exact solutions, the static analysis of multilayer piezoelectric actuators is conducted to show the influence of EMC, the number of piezoelectric layers, the elastic modulus of elastic layer and the thickness ratio on the bending behavior of actuators. The relative error of the tip deflection of a bimorph considering EMC and without considering EMC will be increased to 9.89%. That is to say that the EMC can not be neglected when the piezoelectric coefficient of the material is large enough. One simple formula for the bimorph with considering EMC is given. It is found that the tip deflection is not always increased with the number of layers. It is dependent on the structure of the multimorph. When the effect of the elastic modulus of elastic layers is considered, it is not a good design if only considering the tip deflection of the actuator, but an optimal design can be achieved if the balance between the stress difference and the tip deflection is taken into account. At last, the ratio h_e/h_p is an important factor for the bending behavior of multilayer actuators and the best actuator should be the one with thin elastic layer. In addition, since the material and thickness for different layers may be different in the present investigation, the present work facilitates the modeling and design for different piezoelectric cantilever actuators.

Acknowledgements

This work is supported by the National Natural Science Foundation of China (50272003) and Talent Foundation of Beijing Jiaotong University (2007RC064).

References

Ballas, R.G., Schlaak, H.F. and Schmid, A.J. (2006), "The constituent equations of piezoelectric multilayer bending actuators in closed analytical form and experimental results", *Sensor. Actuat. A-Phys.*, **130**, 91-98.

Brissaud, M. (2004), "Modelling of non-symmetric piezoelectric bimorphs", *J. Micromech. Microeng.,* **14**(11), 1507-1518.

Brissaud, M., Ledren, S. and Gonnard, P. (2003), "Modelling of a cantilever non-symmetric piezoelectric bimorph", *J. Micromech. Microeng.,* **13**(6), 832-844.

Cheng, J.Q., Wang, B. and Du, S.Y. (2005), "A theoretical analysis of piezoelectric/composite anisotropic laminate with larger-amplitude deflection effect, Part I: Fundamental equations", *Int. J. Solids Struct.*, **42**, 6166-6180.

Desmare, R. (1999), "Modeling of multilayer piezoelectric structures", *Ferroelectrics*, **224**(1), 195-202.

DeVoe, D.L. and Pisano, A.P. (1997), "Modeling and optimal design of piezoelectric cantilever microactuators", *J. Microelectromech. S.,* **6**(3), 266-270.

Fernandes, A. and Pouget, J. (2002), "An accurate modelling of piezoelectric multi-layer plates", *Eur. J. Mech. A-Solid.*, **21**(4), 629-651.

Ha, S.K. and Kim, Y.H. (2002), "Analysis of a piezoelectric multimorph in extensional and flexural motions", *J. Sound Vib.*, **253**(5), 1001-1014.

Heyliger, P. and Brooks, S. (1996), "Exact solution for laminated piezoelectric plates in cylindrical bending", *J. Appl. Mech*. ASME, **63**, 903-910.

Huang, C., Lin, Y.Y. and Tang, T.A. (2004), "Study on the tip-deflection of a piezoelectric bimorph cantilever in the static state", *J. Micromech. Microeng.,* **14**, 530-534.

Lee, S.Y., Ko, B. and Yang, W. (2005), "Theoretical modeling, experiments and optimization of piezoelectric multimorph", *Smart Mater. Struct.,* **14**(6), 1343-1352.

Li, S.Q., Liu, Z.X., Zhang, J.G. and Sun, Y. (1999), "Three-dimensional and simplified analysis on static electromechanical mechanism of piezoelectric materials", *J. Shanghai Jiaotong Univ.,* **33**(6), 737-741.

Lin, Q.R., Liu, Z.X. and Wang, Z.L. (2001), "Analysis of beams with piezoelectric actuators", *Appl. Math. Mech.,* **22**(9), 1074-1081.

Liu, M., Tong, J., Wang, L. and Cui, T. (2006), "Theoretical analysis of the sensing and actuating effects of piezoelectric multimorph cantilevers", *Microsyst. Technol.,* **12**(4), 335-342.

Marcus, M.A. (1984), "Performance characteristics of piezoelectric polymer flexure mode devices", *Ferroelectrics*, **57**, 203-220.

Pan, E. (2001), "Exact solution for simply supported and multilayered magneto-electro-elastic plates", *J. Appl. Mech.* ASME, **68**, 608-618.

Pan, E. and Han, F. (2005), "Exact solution for functionally graded and layered magneto-electro-elastic plates", *Int. J. Mech. Sci.,* **43**, 321-339.

Park, S.E. and Shrout, T.R. (1997), "Ultrahigh strain and piezoelectric behavior in relaxor based ferroelectric single crystals", *J. Appl. Phys.,* **82**, 1804-1811.

Shi, Z.F., Xiang, H.J. and Spencer, B.F. (2006), "Exact analysis of multi-layer piezoelectric/composite cantilevers", *Smart Mater. Struct.*, **15**(5), 1447-1458.

Smits, J.G. and Ballato, A. (1994), "Dynamic admittance matrix of piezoelectric cantilever bimorphs", *J. Microelectromech. S.,* **3**(3), 105-112.

Smits, J.G., Dalke, S.I. and Cooney, T.K. (1991), "The constituent equations of piezoelectric bimorphs", *Sensor. Actuat. A-Phys.*, **28**(1), 41-61.

Tadmor, E.B. and Kosa, G. (2003), "Electromechanical coupling correction for piezoelectric layered beams", *J. Microelectromech. S.,* **12**(6), 899-906.

Wang, R.J., *et al*. (1983), *Hand book for marine acoustic materials*, Science Press, Beijing.

Wang, F., Tang, G.J. and Li, D.K. (2007), "Accurate modeling of a piezoelectric composite beam", *Smart Mater. Struct.*, **16**, 1595-1602.

Weinberg, M.S. (1999), "Working equations for piezoelectric actuators and sensors", *J. Microelectromech. S.,* **8**(4), 529-533.

Xiang, H.J. (2007), "Characters of functionally graded piezoelectric smart beams and their applications", Beijing Jiaotong University, PhD, Beijing.

Xiang, H.J. and Shi, Z.F. (2008), "Static Analysis for Multi-layered Piezoelectric Cantilevers", *Int. J. Solids Struct.*, **45**(1), 113-128.

Yang, J. and Xiang, H.J. (2007), "Thermo-electro-mechanical characteristics of functionally graded piezoelectric actuators", *Smart Mater. Struct.*, **16**, 784-797.

Zhou, Y.G., Chen, Y.M. and Ding, H.J. (2005), "Analytical solutions to piezoelectric bimorphs based on improved FSDT beam model", *Smart Struct. Syst.*, **1**(3), 309-324.

JK

Appendix

$$A^{(k)} = \frac{1}{S_{11Ek}} \begin{bmatrix} S_{11P1} & 0 & 0 \\ 0 & S_{11P1} & -\frac{1}{2} g_{311} \end{bmatrix} \tag{A1}$$

$$\tilde{R}^{(k)} = \begin{bmatrix} S_{11Pk} & 0 & 0 \\ 0 & 2S_{11Pk} & -g_{31k} \\ -3g_{31k}(h_{2k}^2 - h_{2k-1}^2) & 2g_{31k}(h_{2k} - h_{2k-1}) & \beta_{33k}(h_{2k} - h_{2k-1}) \end{bmatrix} \tag{A2}$$

$$\begin{pmatrix} k_{11} & k_{12} & k_{13} \\ k_{21} & k_{22} & k_{23} \end{pmatrix} = \sum_{k=1}^{n+1} \begin{bmatrix} -3(h_{2k-1}^2 - h_{2k-2}^2) & 2(h_{2k-1} - h_{2k-2}) \\ -2(h_{2k-1}^3 - h_{2k-2}^3) & h_{2k-1}^2 - h_{2k-2}^2 \end{bmatrix} A^{(k)} + \sum_{k=1}^{n} \begin{bmatrix} -3(h_{2k}^2 - h_{2k-1}^2) & 2(h_{2k} - h_{2k-1}) \\ -2(h_{2k}^3 - h_{2k-1}^3) & h_{2k}^2 - h_{2k-1}^2 \end{bmatrix} B^{(k)} \tag{A3}$$

$$(k_{31}, k_{32}, k_{33}) = (h_2 - h_1)[-3g_{311}(h_2 + h_1), 2g_{311}, \beta_{331}] \tag{A4}$$

$$G_1^{(i)} = (h_{2i} - h_{2i-1})[-3S_{13Pi}(h_{2i} + h_{2i-1}), 2S_{13Pi}, -g_{33i}] \tag{A5}$$

$$G_2^{(i)} = S_{13E,\,i+1} h_{2i}[-3h_{2i}, 2] \tag{A6}$$

$$G_3^{(i)} = S_{13Ei} h_{2i-1}[-3h_{2i-1}, 2] \tag{A7}$$

$$G^{(i)} = G_1^{(i)} R^{(i)} - G_2^{(i)} A^{(i+1)} + G_3^{(i)} A^{(i)} \tag{A8}$$

for $i = 1, 2, \ldots, n$.